Optimization of Dynamic Structured Illumination for Surface Slope Measurements

Guillaume P. Butel[a], Greg A. Smith[a], and James H. Burge[a]

[a]College of Optical Sciences, Univ. of Arizona, 1630 E. University Blvd., Tucson, AZ 85721

ABSTRACT

We present a fast and ambiguity-free method for slope measurement of reflective optical elements based on reflectometry. This novel reflectometric method applies triangulation to compute the slope based off projected patterns from an LCD screen, which are recorded by a camera. Accurate, ambiguity-free measurements can be obtained by displaying one pixel at a time on the screen and retrieving its unique image. This process is typically accelerated by scanning lines of pixels or encoding the information with phase using sinusoidal waves. Various measurement techniques exist, centroiding and phase-shifting being the most accepted, but their sensitivities vary with experimental conditions. This paper demonstrates solutions based on various parameters such as uncertainty or efficiency. The results are presented in a decision matrix and merit function. Additionally, we propose a new measurement technique – Binary squares screens – in an attempt to address system limitations and compare current systems to our solutions using the decision matrix. Several test conditions are proposed along with the best suited solution.

Keywords: Reflectometry, sensitivity, optimization, centroiding, phase-shifting, slopes, structured illumination

1. INTRODUCTION

1.1 Current methods of reflectometry

The reflectometric technique applies Software Configurable Optical Test System (SCOTS) [1] based on a reverse Hartmann test where a monitor (also called screen) projects a structured light pattern that is recorded by a camera, close to the center of curvature (Figure 1). The current test is utilized, for example, in determining the slopes and surface errors for the Giant Magellan Telescope (GMT) and the Large Synoptic Survey Telescope (LSST). The principle behind the software is to geometrically determine the slopes of an optical element, using

$$w_x = \frac{\dfrac{x_{mirror} - x_{screen}}{z_{mir2screen}} + \dfrac{x_{mirror} - x_{camera}}{z_{mir2camera}}}{2} \tag{1}$$

for the slopes in the x axis. x_{mirror} (respectively x_{camera}) designates the x coordinate of the distance from the center of the screen to the mirror vertex (respectively the camera aperture stop). x_{screen} is the x coordinate of the screen pixel calculated from the screen center that illuminates the mirror at the considered location. $z_{mir2screen}$ ($z_{mir2camera}$) is the z coordinate of the distance from the screen to the vertex (the camera aperture stop). The details of the geometry can be found in Figure 1. A similar formula is used for the y axis, where x becomes y. We use the approximation that the sag is small compared to the distance z. The above formula allows calculating the slopes using three locations: mirror, screen, and camera aperture stop. The profile can then be integrated from the slopes using different techniques, which will not be described in this paper.

Each mirror pixel is uniquely associated with a screen pixel. For a given mirror pixel, the screen pixel location is the only unknown geometric variable after knowing the geometry of the test (camera, screen and mirror positions). A complete description of the process with examples is given by Su et al. [1]. Centroiding and phase-shifting (PS) are the two main measurement techniques currently used to retrieve the screen pixel location x_{screen} and thus the slope information.

In this paper, we propose a third measurement technique, called "Binary squares screens", which mitigates issues seen in the two standard solutions. We compare the different measurement techniques according to various parameters (uncertainty, precision, efficiency, etc…) and then build a matrix that summarizes and ranks the solutions. We also present the design of a merit function to represent the conditions of the optical test. The merit

function provides a set of coefficients that alter the ranking between the different solutions and reveals the best suited solution depending on test conditions.
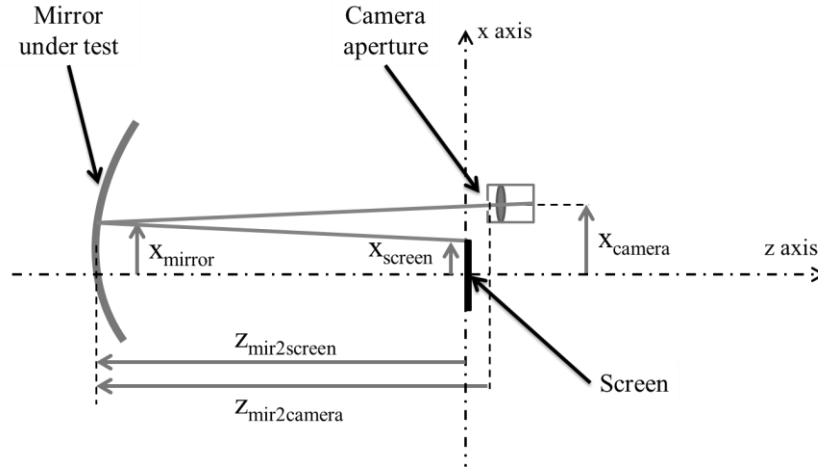

Figure 1. SCOTS geometry. Light propagates from the screen onto the mirror but only the screen pixels conjugate with the stop for a given mirror pixel are recorded by the camera.

1.2 Phase-shifting

Phase-shifting methods use light modulation: the light intensity on the screen (or the pixel brightness) is modulated by a sinusoidal function that is then shifted several times by a certain fraction of its period, which allows retrieving the phase of the sine pattern at any point on the screen. The sinusoidal function is typically shifted four times by $\pi/2$. The phase retrieval utilizes the four intensities recorded for each phase shift, at a given mirror location. Therefore, we can associate a phase value to each mirror pixel using

$$\Phi = \arctan\left[-\frac{I_2 - I_4}{I_1 - I_3}\right] \tag{2}$$

to retrieve the phase and thus the coordinates of the active screen pixel during the process. This four step phase-solving algorithm described by Wyant [20] and Schwider [3] is used in classic interferometric testing [4-7]. More advanced phase-shifting methods were developed to reduce the error caused mainly by detuning of phase shifter [8-10]. The five- [8, 9], six- [9, 10] and seven-step [9] phase-shifting algorithms may have a higher insensitivity to noise but require longer acquisition time. All the phase-shifting methods have a similar limitation known as 2π ambiguity. This ambiguity occurs when multiple fringes (i.e. multiple times 2π) are used to map optical elements, causing two mirror pixels on the optic to have the same calculated phase even though they do not in actuality. A process known as phase unwrapping is required to retrieve the real phase information (Figure 2).
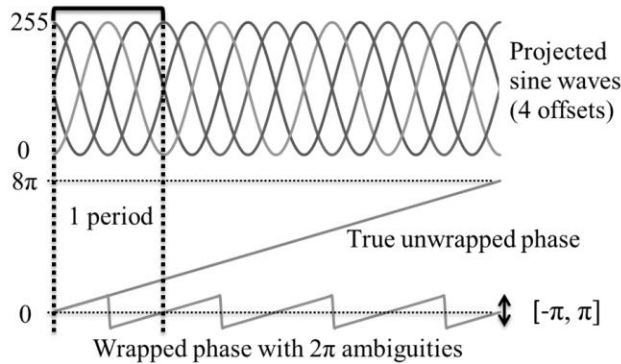

Figure 2. Phase-shifting phase inherent issue: phase unwrapping. The displayed sine fringes (above) converts the screen locations into 8π-phase and intensity patterns. Four pictures are taken to reconstruct the phase at a given location on the mirror but the period on the original sine wave is unknown and unwrapping is required to calculate the true screen location.

Once the phase is correctly calculated, the screen pixel location r$_{screen}$ is obtained geometrically using

$$r_{screen} = \frac{\Phi N}{2\pi n} \tag{3}$$

where Φ is the calculated phase, N is the total number of pixel and n is the number of periods displayed. We use r$_{screen}$ for the screen pixel location in order to have a generic name for x and y, because the calculations are identical for both cases. If N is in pixels, then r$_{screen}$ is in pixels too. However, N can be converted in mm using the pitch of the screen.

1.3 Centroiding

The centroiding measurement techniques display black and white patterns on the screen and do not apply phase components to retrieve screen pixel information. For a single illuminated pixel, the camera observes a bright spot for slopes that satisfy specular reflection conditions where centroiding locates these specular reflection points. To accelerate processing, an x-y line scanning method is typically used to illuminate many points at once, where lines first scan in the x and then y dimensions. The intensity reaches a maximum for a specific screen pixel and then decreases as the pixel line moves past, thus locating the intensity profile for each mirror pixel (Figure 3). The intensity varies as a function of the screen coordinates and a centroiding algorithm then calculates the position of the maximum using

$$x_m = \frac{\sum I_i x_i}{\sum I_i} \text{ and } y_m = \frac{\sum I_i y_i}{\sum I_i}. \tag{4}$$

The calculated position is then applied to the slope equation (Eq. 1), which is common to all the given methods. Acquisition time for centroiding is longer than phase-shifting for two main reasons: 1) one picture corresponds to one line position and 2) the area that needs to be scanned has to be bigger than the minimum area required to illuminate the whole optic. The second reason is necessary to obtain a symmetric intensity function, including the tails that go to zero (or background noise level), as shown in Figure 3.
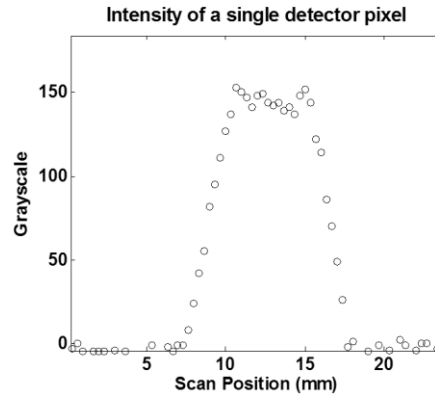

Figure 3. Pixel intensity function during line scanning. The width w of the function is the sum of the aperture stop diameter and the size of the light spot on the screen.

1.4 Summary of existing methods

For clarity, we propose a summary table which shows the important steps for the SCOTS process as a whole. The difference between phase-shifting and centroiding are also included. The variable r is a generic variable to represent x or y, because their calculation is identical.

Table 1. SCOTS process scheme

Setup	Setup the system, measuring geometry ($r_{mirror}, r_{camera}, z_{mir2screen}, z_{mir2camera}$)
Data acquisition	Screen display
	Camera acquisition or picture taking
Data	Create a mask for the optic

reduction	CENTROIDING	PHASE-SHIFTING
	Threshold the intensity maps	Phase unwrapping $$\Phi = \arctan\left[-\frac{I_2 - I_4}{I_1 - I_3} \right]$$
	$$r_{screen} = \frac{\sum I_i r_i}{\sum I_i}$$	$$r_{screen} = \frac{\Phi N}{2\pi n}$$
	Slopes calculation $$w_r = \frac{\dfrac{r_{mirror} - r_{screen}}{z_{mir2screen}} + \dfrac{r_{mirror} - r_{camera}}{z_{mir2camera}}}{2}$$	
	Slope fitting and integration (not considered here)	

2. SYSTEM PERFORMANCE PARAMETERIZATION

Our goal is to select the most optimized method for measurements when given certain conditions. For this purpose, standard parameters need to be introduced and properly defined. We propose the use of seven parameters, whose definitions follow: uncertainty, precision, equipment needed, processing time, noise tolerance, acquisition time, and calibration. Each method will be analyzed according to those seven parameters. Some parameters are quantitative, such as uncertainty or precision, and others are qualitative, such as the equipment needed. The qualitative parameters are ranked on a 7-level scale, 1 being the worst possible score and 7 the best. As an example, a method that requires a very powerful computer to function would be ranked as 1 or 2. Some common parameters have to be fixed in order to compare solutions of the various systems on a fair basis:

- Uncertainty is the difference between the obtained values relative to a reference value, which is linked to systematic errors. We compare the measurements to an external value, which we call reference value. Practically, we compare the expected value to the simulated value in the presence of noise, defined below.
- Precision, or repeatability, is the deviation between all the obtained results (standard deviation). . The precision is relative to a measure itself. We compare the measurements between themselves when run with different random noises. Errors are detailed for each method and the precision is defined by the superposition of those errors.
- Equipment needed defines the quality of the screen and camera. There is a wide range of equipment that can be used for testing. The standard numbers for the equipment that we are using are a pixel pitch of 200 microns, and a screen size of 200x200 pixels. The screen displays intensity levels that can be coded on 8 bits, i.e. the intensity values vary from 0 to 255. The aperture stop of the camera is 2 mm in diameter. The quality of the screen is not critical for any of the methods since standard screens have a high optical quality but the quality of cameras can vary from low-grade consumer products to high-end scientific cameras (Point Grey Research™). Integrated cameras, like webcams, have an automated algorithm that control their gain or shutter. If the linearity is not much worse than scientific cameras, their lack of control makes the calculations somewhat difficult. Control on parameters such as gain, and shutter speed are therefore important. Any camera has to be corrected from distortion because it can cause large systematic errors, and it is not difficult to correct.
- Processing time and computation overhead. This is a rather qualitative metric to be able to classify the solutions according to the available computation resources. The standard that we use is a laptop with an Intel® Core i5™-2410M processor at 2.3 GHz with a particular algorithm implemented in MATLAB. The algorithms have not been optimized but provide an approximate relative measure of performance.
- Noise tolerance defines how the system performs in a noisy environment. Under various levels of noise, we analyze how the uncertainty scales. The standard noise has been chosen to be 2% of 256 (8 bits), and we will analyze the behavior at 2%, 10% and 20% of noise. The noise is uniform in the interval [-5; 5], with σ_i = 2.88. A uniform distribution has been chosen over a Gaussian distribution.
- Acquisition time is the time the solution needs to acquire all the pictures to calculate the slopes. The standard time we consider to acquire a picture is 0.1 s.

- Calibration is a qualitative metric to estimate the importance of calibrating the method before data collection. As stated above, the distortion of the camera has to be corrected. The screen linearity and uniformity are two parameters that may have to be calibrated, depending on their deviation from a good quality standard.

The integration process is common to all the methods and will not be taken into account. Some parameters such as calibrating the camera are common to all methods within a measurement technique and will be discussed within the technique itself.

3. MEASUREMENT TECHNIQUES

Three measurement techniques will be described in this section: the centroiding technique, the phase-shifting technique and the Binary Squares screen technique. For each technique, we will give various possible solutions and define them in terms of the previously stated parameters.

3.1 Centroiding measurement techniques

All centroiding measurement techniques apply the same formula (Eq. 4) to calculate the best screen position for a given mirror pixel. However the displayed screen pattern can be altered to create various solutions and address different needs. A dot being scanned across the screen is the simplest centroiding solution, but this solution acquires data very slowly. A second solution, also the most accepted, is a line scanning across the screen. A third solution that we would like to introduce is a square scanning approach. Square scanning appears similar to dot scanning but is faster with higher SNR due to the use of many more pixels. These three methods constitute our group of solutions for centroiding with the following defined parameters:

Table 2. Centroiding methods inputs

	Dot scanning	Line scanning	Square scanning
Size (pixels)	2x2	4x200	10x10
SNR	50	100	100
w (pixels)	12	14	20
N	12	14	20
Scanning rate	1 pixel/frame	2 pixels/frame	2 pixels/frame
Total number of pictures (x & y)	>2000	400	>2000

N is the number of sampling points higher than the noise level and w the width of the intensity function (w is also equal to the sum of the width of the light pattern on the screen and the width of the aperture stop). Knowing the width of the stop in mm, we can convert it in pixels using the pixel pitch.
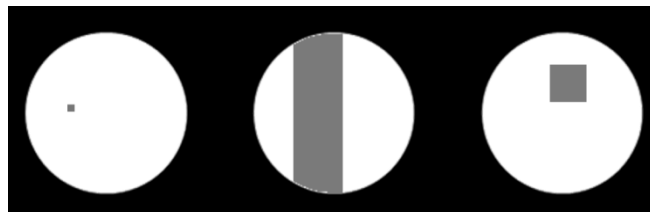

Figure 4. Scheme showing the three different solutions, as seen through the camera aperture stop (not to scale)

In general, centroiding methods [1] are:

- Insensitive to light variations in temporal domain (intensity varies between different mirror pictures)
- Sensitive to light variations in spatial domain (intensity varies between different pixels on one picture)

They have a good SNR because they are using the maximum light intensity at each screen pixel. They require a high spatial light uniformity, usually achieved by monitors. They do not get errors from fringe overlapping as one line is used at a time for reducing the data. Dot scanning is not sensitive to light variations in spatial domain due to

The precision for centroiding is based on 5 parameters: noise (source, camera), aperture radius (stop size), line width (should be close to stop size), pixel separation error, vibration (air, camera, sensor). We estimate the precision [11] to be

$$\sigma_p = \frac{w}{2 \cdot \sqrt{N} \cdot SNR} \tag{5}$$

where w is the total width at the noise level of the intensity function (shown in Figure 3), N the number of samples, and SNR the signal-to-noise ratio. In this model, we neglect the vibration errors and pixel separation errors.

The centroiding methods usually have a good SNR (SNR > 50) because they use maximum light intensity at each screen pixel during data acquisition [12]. The width of the intensity function depends on the camera stop size and the line width on the screen. Ideally the two parameters should be close in dimensions. If the width of the centroiding is set to 20 pixels, and the SNR to 100, the precision is then 0.007 pixels or 1.4 microns.

The uncertainty is based on the intensity uniformity on the screen because we use different locations on the screen for each location that needs to be determined. The screen uniformity or the intensity fluctuations can affect the measurement. As previously stated, we use a uniform noise at 2% of the 256 levels. Figure 5 shows the ideal intensity response with a black line and a response altered by noise with grey dots. By comparing the two results, we can estimate the uncertainty of the solution.
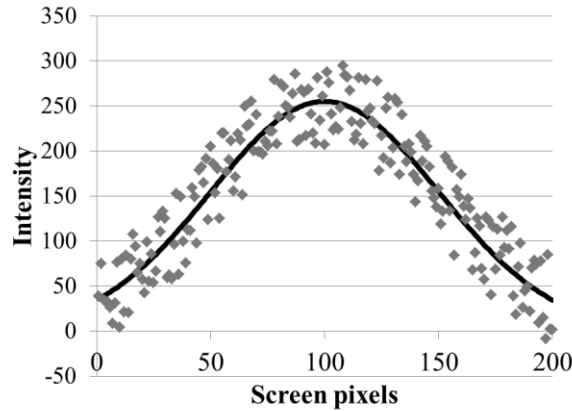

Figure 5. Noise in centroiding detection showed in the intensity function

The equipment needed for centroiding techniques can be of standard quality for several reasons. They require spatial intensity uniformity but it is usually achieved on a small region of the screen, even if the monitor does not have a uniform intensity output over its entire size. All the 3 methods in this technique will have the same ranking.

The processing time is fairly quick because the calculations required by the centroiding algorithm are not very demanding. All the 3 methods require about the same processing time. According to experiments made in the lab, we need about 180s to analyze 60 pictures in order to get the slopes using Eq. 1.

To analyze the noise tolerance, we increase the noise level to 2%, 10% and 20% and we look at the uncertainty change. The noise tolerance is fairly good for line scanning and square scanning. The uncertainty of the dot scanning goes up to almost 30 μm under 20% of noise (Figure 6).
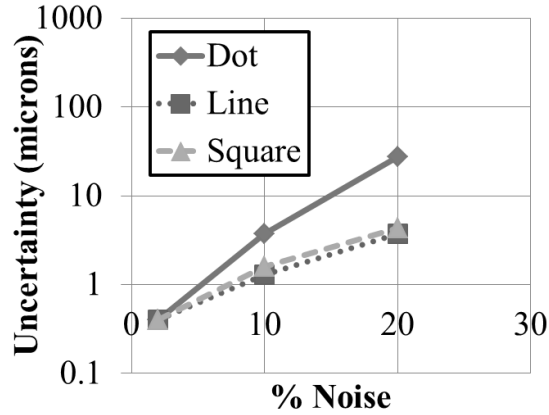
Figure 6. Noise tolerance for the centroiding methods (the y axis is plotted in log scale)

The acquisition time is about 20s for line scanning. Taking one picture takes about 0.1s. We have 200 pictures to take for the line scanning to cover x and y, which leads to 20s. We could increase the rate to 4 pixels per frame to reduce the time but the precision would be worse. The rate (in pixels per frame) expresses the number of pixels between 2 pictures, the minimum being 1. The smaller rate, the longer time we need, but the better precision (higher N) we obtain. The rate is a parameter in the code and can be adjusted by the operator. Finally, calibration is not critical for centroiding and we will set the same value for all the methods.

We summarize the results for the 3 different solutions in the following table:

Table 3. Centroiding parameters summary

Solution	Dot scanning	Line scanning	Square scanning
Uncertainty	1 μm	1 μm	1 μm
Precision	6.9 μm	3.7 μm	4.4 μm
Equipment needed	4	4	4
Processing time	4	4	4
Noise tolerance	27 μm	4 μm	4 μm
Acquisition time	>200s	20s	>200s
Calibration	4	4	4

3.2 Phase-shifting measurement techniques

Phase-shifting solutions use various formulae to calculate the location of the screen pixels. The formulae depend on the number of steps used in the phase-shifting process, which can range from 3 to 7 usually, 4 steps being the most common. More steps mean a better tolerance to noise, as shown in various papers [8-10]. The formula (Eq. 1) describes a four-step process, and using more phase steps would increase the number of intensity values to be considered, as shown in (3) for a 6-step algorithm [10]:

$$\Phi = \arctan\left[\frac{-3I_2 + 4I_4 - I_6}{I_1 - 4I_3 + 3I_5}\right]$$

(6)

As opposed to centroiding, phase-shifting methods are [1]:

- Sensitive to light variations in temporal domain (intensity varies between different mirror pictures)
- Insensitive to light variations in spatial domain (intensity varies between different pixels on one picture)

Therefore they are not affected by screen non-uniformity, the linearity is however important. The equipment for phase-shifting has to be better than average to ensure the correct phase encoding and decoding. Finally, phase-shifting techniques have to choose between contrast and sensitivity. The more periods are used in the sine wave, the less contrast the image will have but the more sensitive the solution is. This is even more critical when working in a noisy environment because the noise level will lower the cut-off frequency of the system, and possibly will make

impossible the use of high frequency waves. Multiple phase shifting patterns could be used at the expense of increased time and processing.

Phase-unwrapping is necessary when multiple periods are used to encode the light intensity. Many unwrapping algorithms exist [13, 14], but they require extra time and resources to get the correct phase. Phase-shifting do require better resources than centroiding to calculate the screen positions.

There are several error sources for phase shifting algorithms [13, 15]:

- Vibrations: Vibrations in the setup can introduce errors because the camera can image a mirror pixel illuminated by a wrong screen pixel onto the sensor and lead to a wrong phase. We will assume that the vibrations add a common phase error of 4.5 mrad, which corresponds to 7.1 microns on our screen.
- Quantization errors: The digitization of the intensity information from the detector to the computer may have some errors depending on how many bits and steps are used. The formula derived by Brophy [16] gives the standard deviation of this error

$$\sigma_q = \frac{2}{\sqrt{3n}\,2^b} \tag{7}$$

  as a function of the number of bits b and phase steps n used. The error is in radians. The quantization error is very small, once the SNR is above 5-10.

- Screen intensity fluctuations: The screen intensity can vary or flicker and we represent this variation with the standard deviation of the uniform law for 2% noise, as described in section 1. The standard is 2.88 out of 256 intensity levels for this error.
- A thorough discussion of uncertainties in phase-shifting formulae has been made by Hack and Burke [15]. Their results will be added to this discussion in the future.

For our comparison group, we will use 4 solutions from the phase-shifting technique: 3-step, 4-step, 6-step and 4-step with a 5th screen to get rid of the phase ambiguity. This new solution adds a 5th pattern to the existing 4 to be able to know on which period the pixel is. Knowing this piece of information, the unwrapping is very quickly done, as the phase offset can be written $2\pi(p-1)$ where p is the period number (p ≥ 1). This 5th screen is a linear function of 256 levels over the entire screen used. This guarantees the unique relation between a mirror pixel location and a screen pixel. In case of the non-uniformity or linearity of the display, more patterns can be added to average out the noise and a better screen calibration could also be implemented. The linearity is, in that case, very important because it guarantees the proper numbering of the sinusoidal periods used. It is thus critical to know the screen's response.

Table 4. Phase-shifting methods inputs

Solutions	3-step	4-step	6-step	4-step +slope
Phase retrieval formula	$\Phi = \tan^{-1}\left[\dfrac{-I_2 + I_3}{I_1 - I_2}\right] + \dfrac{\pi}{4}$	$\Phi = \tan^{-1}\left[\dfrac{-I_2 + I_4}{I_1 - I_3}\right]$	$\Phi = \tan^{-1}\left[\dfrac{-3I_2 + 4I_4 - I_6}{I_1 - 4I_3 + 3I_5}\right]$	Same as 4-step
Unwrapping algorithm	Yes	Yes	Yes	No
Number of pictures	6	8	12	10
Period number	10	10	10	10
SNR	30	30	30	30

The number of pictures needed for each solution takes into account the fact that we have to scan in x and y, so for example 3-step requires 3 pictures per dimensions, so 6 total for x and y.

The precision for a phase-shifting solution is a root square sum of the precisions we stated above. We consider the intensity fluctuations and the quantization error in our calculation. The uncertainty of phase-shifting will be calculated like the one for centroiding, using a uniform noise for the intensity distribution. The processing time may vary from a phase-shifting to another but the unwrapping is the most time-consuming task to do. It strongly depends

on algorithms and how they are implemented. Because the 5th phase-shifting method is unwrapping free, the processing time is greatly reduced. The acquisition time is fairly quick because 12 pictures are taken at most, which we calculated to be 1.2s.

The equipment needs to be better than for centroiding because the screen has to have a good linearity, as the intensity uncertainty suffers from nonlinearity. Calibration may therefore be necessary for the screen. The noise tolerance is calculated in the same manner as for centroiding (Figure 7):
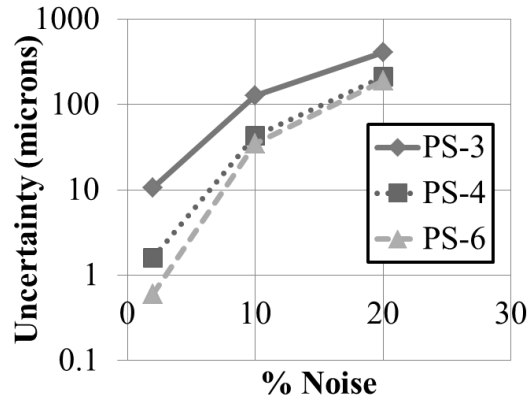

Figure 7. Noise tolerance for the phase-shifting methods (the y axis is plotted in log scale)

As stated above, screen calibration may be necessary. All phase-shifting methods will be ranked the same way because the calibration is necessary for all of them.

The summarized results for the phase-shifting methods are available in Table 5.

Table 5. Phase-shifting methods parameters

Solutions	3-step	4-step	6-step	4step+slope
Uncertainty	11 μm	1.6 μm	0.6 μm	3 μm
Precision	7.5 μm	6.9 μm	5.9 μm	7.2 μm
Equipment needed	3	3	3	3
Processing time	4	4	4	7
Noise tolerance	408 μm	213 μm	188 μm	213 μm
Acquisition time	0.6s	0.8s	1.2s	1s
Calibration	3	3	3	3

3.3 Binary squares screens solutions

We would like to propose a novel technique that is using very low resources and standard quality equipment. This technique is still at the concept stage and it will be described in more details in a future paper. This concept has been developed to address some drawbacks of the two other techniques like the unwrapping uncertainty, the computational power, and the processing time. It can take time, with the other methods, to have a first result from the acquired data. With this new method, we want something flexible that can be stopped anytime if the operator wishes so. It should also not require a lot of calculating resources. We call it "Binary squares screens" technique because the screens display a pseudo-random pattern of black and white squares (Figure 7).
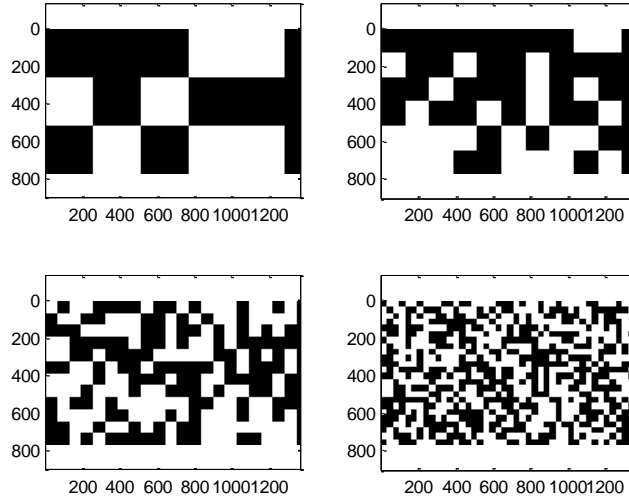
Figure 8. Binary squares screen display

The goal of this new technique is to adapt to the optic that needs to be measured, to require less processing time and resources, and to maintain accurate results. The slope retrieval is based on centroiding. Each mirror pixel is first illuminated by a black or white pixel. From this, we can calculate the slopes with a lot of ambiguity because several white pixels are present on the screen and we have no means to distinguish them. Then a second screen is displayed with twice smaller squares and the slopes can be calculated with less ambiguity. The process continues until the operator obtains the resolution he desires (Figure 8). In the perfect case, each mirror pixel is associated with a unique series of 0 (black square) and 1 (white square).

For this new method, the precision depends on the size of the squares, the SNR and the number of screens displayed. We estimate the precision to be 20 microns because of the size of the squares that vary from 200 to 25 pixels or less. The SNR is estimated to be similar to the one for centroiding, 50. The uncertainty depends on the intensity fluctuations, the uniformity of the screen, and the ambiguity of the pattern. After the first screen, there are a lot of ambiguities and the uncertainty is thus high. The more screens are used, the lower the uncertainty goes. We estimate it to be 5 microns. Since the centroiding methods use the same kind of binary intensity levels, the noise tolerance is estimated to be close to the one of those.

As far as the qualitative parameters go, centroiding is a good starting point but this new method differs on some aspect. We want to be able to use a wide variety of equipment for this method: from low-end cameras to high quality screens, this method is designed to be used on almost any kind of support. Its processing time is fast, on the order of seconds. Its acquisition time varies depending on the optic and the uncertainty/precision required. The rank that we will attribute will be 3 because the uncertainty and precision are becoming acceptable only after a significant number of screens displayed. Finally, calibration is similar to centroiding, so the same qualitative arguments apply.

Table 6. Binary screens parameter estimates

Solution	Binary squares screens
Uncertainty	5 μm
Precision	20 μm
Equipment needed	5
Processing time	6
Noise tolerance	200 μm
Acquisition time	1s
Calibration	4

The values listed in the above table are estimates.

4.   DECISION MATRIX AND MERIT FUNCTION

We can gather all the results in a single matrix that we call a decision matrix. For each parameter, the best value (highest or lowest depending on the parameter) will be attributed the value 7 and the worst 1. The intermediate values are scaled accordingly and rounded to the nearest integer.

Table 7. Decision Matrix

Parameters	Dot scanning	Line scanning	Square scanning	3-step PS	4-step PS	6-step PS	4-step + slope PS	Binary squares
P1-Uncertainty	7	7	7	1	6	7	6	4
P2-Precision	6	7	7	6	6	6	6	1
P3-Equipment needed	4	4	4	3	3	3	3	5
P4-Processing time	4	4	4	4	4	4	7	6
P5-Noise tolerance	7	7	7	1	4	4	4	4
P6-Acquisition time	1	6	1	7	7	7	7	7
P7-Calibration	4	4	4	3	3	3	3	6

With this decision matrix, we need a merit function to decide which one of the solutions is the best suited for specific conditions. The merit function will assign weights to each of the parameters depending on the conditions of the test and on which parameters the operator wants to emphasize for his test.

$$Merit(j) = \sum_{k=1}^{7} a_k M(k, j) \tag{8}$$

where the vector a contains the weights assigned by the operator and M contains the coefficients of the decision matrix. j (from 1 to 7) indicates which solutions the merit function is calculated for. Each weight is chosen between 1, 2, 3, and 4 (4 meaning most important and 1 the least).

From the decision matrix, we can directly see that centroiding methods and phase-shifting with steps higher than four have the best precision and uncertainty. If the weighting coefficients are equal, then line scanning is the best method, followed by the 4-step phase-shifting with an extra screen.

If we consider different situations, the first one will be people doing a presentation at an outreach event in a high-school, the second a quick demo at a conference and the third one, scientists working in a lab and desiring to measure an optic. All of those conditions have different goals, expectations and thus require a different set of coefficients a. We need to convert those "real test conditions" into numbers that will feed our merit function and give us our optimal method for our test. Giving a presentation in front of a class of high-school students require a fast and efficient method, using the basic equipment that can be available in the classroom. The weights for speed, equipment and processing have to be emphasized. In this case, we apply a score of 4 to the coefficients P3, P4, P6, and P7 and we find that the binary squares screens are the best suited method for this application. We can reproduce this method for any test conditions.

5.   CONCLUSION

In this paper, we demonstrated that it is possible to find a best suited solution for measuring the slopes of an optic by reflectometry. We first presented different solutions among centroiding and phase-shifting and detailed their sensitivities according to 7 parameters (like uncertainty, precision, processing time, or noise tolerance). We introduce a new phase-shifting method, which can achieve comparable results to other phase-shifting methods but without having the need of an unwrapping algorithm. We then proposed a new method, based on centroiding, but that could be used on lower-end computing resources and adapted to the optic itself by deciding when to be stopped. After each projected screen, a calculation is made and the operator can decide to pursue the process or to stop it, if he is satisfied with the result. Finally, we gathered all the results in a decision matrix to have a broader view of the

sensitivities of all the 8 methods presented in the paper. A merit function is also proposed in order to optimize the decision of the best method suited to the test conditions. The best method for a quick measurement is the binary squares screens. The best method for a noise tolerant and quick calculation is 4-step + linear screen phase-shifting. The best method for a precise and accurate measurement is line scanning centroiding.

6.   REFERENCES

[1] Su P., Parks R. E., Wang L., Angel R. P. and Burge J. H., "Software configurable optical test system: a computerized reverse Hartmann test," *Applied Optics*, 49, 25 (2010)

[2] Wyant J. C., "Interferometric optical metrology: basic systems and principles," *Laser Focus,* 65-71 (1982)

[3] Schwider J., "Detection of undersampling from measured phase-shifting data," *Optics Letters,* 19, pp. 231-233 (1994)

[4] Creath K., "Phase-Measurement Interferometry Techniques," in Wolf E. (Ed.): *Progress in Optics XXVI*, pp. 348–393, Elsevier Science Publishers B.V., Amsterdam (1988)

[5] Greivenkamp J. E., Bruning J. H., "Phase Shifting Interferometry," in Malacara D. (Ed.): *Optical Shop Testing*, Third Edition, pp. 501–598, John Wiley, New York (2007)

[6] Vlad V. I., Malacara D., "Direct Spatial Reconstruction of Optical Phase from Phase-Modulated Images," in Wolf E. (Ed.): *Progress in Optics XXXIII*, pp. 261–317, Elsevier Science Publishers B.V., Amsterdam (1994)

[7] Malacara D., Servin M., Malacara Z., "Interferogram Analysis for Optical Testing," Marcel Dekker, Inc., New York (1998)

[8] Novák J., "Five-step phase-shifting algorithms with unknown values of phase shift," *Optik,* 114, No. 2, pp. 63-68 (2003)

[9] Novák J., Novák P., Miks A., "Multi-step phase-shifting algorithms insensitive to linear phase shift errors," *Optics Communications,* 281, pp. 5302-5309 (2008)

[10] Schmit J., and Creath K., "Extended averaging technique for derivation of error-compensating algorithms in phase-shifting interferometry," *Appl. Opt.,* 34, 3610-3619 (1995)

[11] Su T., Park W. H., Parks R. E., Su P., and Burge J. H., "Scanning Long-wave Optical Test System – a new ground optical surface slope test system," *Proc. SPIE*, 8126, pp. 81260E-81260E-10 (2011)

[12] http://www.optics.arizona.edu/jcwyant/Optics513/ChapterNotes/Chapter05/2-PHASE SHIFTING INTERFEROMETRY.pdf

[13] Winick K. A., "Cramer–Rao lower bounds on the performance of charge-coupled-device optical position estimators," *J. Opt. Soc. Am. A,* 3, 1809–1815 (1986)

[14] Osten W., Nadeborn W., and Andrä P., "General hierarchical approach in absolute phase measurement," *Proc. SPIE,* 2860, 2–13 (1996)

[15] Hack E., and Burke J., "Measurement uncertainty of linear phase-stepping algorithms," *Rev. Sci. Instrum*., 82(6), 061101 (2011)

[16] Brophy C. P., "Effect of Intensity Error Correlation on the Computed Phase of Phase-Shifting Interferometry," *J. Opt. Soc. Am. A*, 7, 537 (1990)